Inorganic Chemistry
Article

Inorg. Chem. **2011**, *50*, 517–524 **517**
DOI: 10.1021/ic101629w

Mononuclear and Dinuclear Ruthenium Complexes of 2,3-Di-2-pyridyl-5,6-diphenylpyrazine: Synthesis and Spectroscopic and Electrochemical Studies

Yu-Wu Zhong,*,† Si-Hai Wu,† Stephen E. Burkhardt,‡ Chang-Jiang Yao,† and Héctor D. Abruña*,‡

†*Beijing National Laboratory for Molecular Sciences, CAS Key Laboratory of Photochemistry, Institute of Chemistry, Chinese Academy of Sciences, Beijing 100190, People's Republic of China, and* ‡*Baker Laboratory, Department of Chemistry and Chemical Biology, Cornell University, Ithaca, New York 14853-1301, United States*

Received August 10, 2010

Reported here are a new bridging ligand, 2,3-di-2-pyridyl-5,6-diphenylpyrazine (dpdpz), and its complexation with one or two ruthenium atoms. This ligand was designed so that it could bind to metal species in either a N^N bidentate fashion or a C^N^N tridentate mode to form a metallacycle. The reaction between dpdpz and $(tpy)RuCl_3$ (tpy = 2,2′:6′,2″-terpyridine) afforded C^N^N-type mono- and dinuclear cyclometalated complexes in moderate yields. On the other hand, N^N-type mono- and dinuclear noncyclometalated complexes could be isolated from the reaction of dpdpz with $(bpy)_2RuCl_2$ (bpy = 2,2′-bipyridine). An asymmetric diruthenium complex, bridged by dpdpz, was prepared with one ruthenium atom cyclometalated and another one noncyclometalated. The electronic properties of these complexes were probed by electrochemical and spectroscopic techniques. They exhibited multiple reversible redox processes. However, the formal potentials and electrochemical energy gap are greatly dependent on the binding nature and number of ruthenium atoms. As indicated by electrochemical and spectroelectrochemical studies, diruthenium complexes bridged by dpdpz exhibited electronic coupling between the two metal centers. A comparison of the electronic absorption and emission properties of these complexes is also presented.

Introduction

Because of their appealing photophysical and electrochemical properties, transition-metal polypyridine complexes have been extensively employed for building macromolecular assemblies and molecular wire prototypes.[1] Complexation of transition metals with polypyridine ligands provides molecular structures with rigid and well-defined geometries. Optimal orbital overlap between metals and organic ligands gives rise to electronic delocalization along the entire molecule. This narrows the highest occupied molecular orbital (HOMO)−lowest unoccupied molecular orbital (LUMO) gap and gives rise to intense absorption in the visible region of the spectrum. These properties make transition-metal polypyridine complexes attractive building blocks for the construction of molecular architectures to perform light and redox-related functions.

A simple, deliberate, and general way to construct polynuclear coordination oligomers or polymers is to assemble metal centers using appropriate bridging ligands. In this sense, one of the most extensively studied polypyridine bridging ligands, 2,3,5,6-tetra-2-pyridylpyrazine (tppz; Figure 1), has been shown to yield a great number of linear and rigid molecular assemblies when bound to octahedral transition-metal ions such as Fe^{II}, Ru^{II}, Os^{II}, and Co^{II} in a bis-terdentate fashion.[2] These compounds exhibit a high degree of electronic coupling and are most attractive for the generation of highly conductive one-dimensional molecular wires because of the extended π conjugation and their ability to mediate electron transfer through multiple redox states of the transition metals. Unfortunately, these complexes are mostly nonemissive at room temperature. In comparison, polynuclear Ru^{II}, Os^{II}, Re^{I}, and Cu^{I} complexes based on the bidentate bridging

*To whom correspondence should be addressed. E-mail: zhongyuwu@iccas.ac.cn (Y.-W.Z.), hda1@cornell.edu (H.D.A.).

(1) (a) Schubert, U. S.; Eschbaumer, C. *Angew. Chem., Int. Ed.* **2002**, *41*, 2892. (b) Harriman, A.; Ziessel, R. *Chem. Commun.* **1996**, 1707. (c) Balzani, V.; Juris, A.; Venturi, M. *Chem. Rev.* **1996**, *96*, 759. (d) Barigelletti, F.; Flamigni, L. *Chem. Soc. Rev.* **2000**, *29*, 1. (e) Ziessel, R. *Synthesis* **1999**, 1839. (f) Balzani, V.; Juris, A. *Coord. Chem. Rev.* **2001**, *211*, 97. (g) Eryazici, I.; Moorefield, C. N.; Newkome, G. R. *Chem. Rev.* **2008**, *108*, 1834. (h) Constable, E. C. *Chem. Soc. Rev.* **2007**, *36*, 246. (i) Medlycott, E. A.; Hanan, G. S. *Chem. Soc. Rev.* **2005**, *34*, 133. (j) Baranoff, E.; Collin, J.-P.; Flamigni, L.; Sauvage, J.-P. *Chem. Soc. Rev.* **2004**, *33*, 147.

(2) (a) Arana, C. R.; Abruña, H. D. *Inorg. Chem.* **1993**, *32*, 194. (b) Chanda, N.; Sarkar, B.; Kar, S.; Fiedler, J.; Kaim, W.; Lahiri, G. K. *Inorg. Chem.* **2004**, *43*, 5128. (c) Hartshom, C. M.; Daire, N.; Tondreau, V.; Loeb, B.; Meyer, T. J.; White, P. S. *Inorg. Chem.* **1999**, *38*, 3200. (d) Dattelbaum, D. M.; Hartshom, C. M.; Meyer, T. J. *J. Am. Chem. Soc.* **2002**, *124*, 4938.

Published on Web 12/09/2010

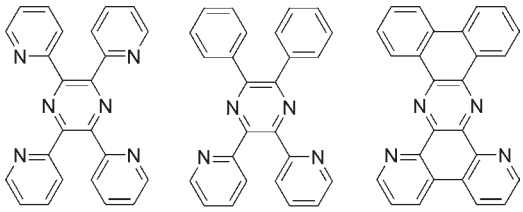

Figure 1. Bridging ligands.

ligands 2,3-di-2-pyridylpyrazine (dpp), 2,3-di-2-pyridylquinoxaline (dpq), and 2,3-di-2-pyridylbenzo[*g*]quinoxaline (dpb) and their derivatives are emissive.[3] Most of these complexes absorb strongly and emit in the vis/near-IR (NIR) region. They have been investigated in many photoinduced energy/electron-transfer processes and as light-harvesting materials. All of these studies have demonstrated that the development of new polypyridine bridging ligands with comparable and complementary electronic properties is still of great interest to the materials science and chemistry communities.[4]

Recently, much attention has been paid to cyclometalated ruthenium complexes, which have at least one Ru−C σ bond present in the complex. The introduction of a negative charge in the ligand strongly affects the electronic and photophysical properties of the complexes. In contrast to noncyclometalated counterparts, cyclometalated ruthenium complexes generally exhibit much lower metal-based oxidation potentials[5] and stronger metal−metal electronic coupling between individual metal centers.[6] It should be noted that bis(triazole)- or bis(tetrazole)pyridine, as reported by Vos and co-workers, can also act as σ-donor ligands, and the corresponding Ru^{II}(tpy)-type complexes show attractive emissive properties.[7] However, detailed comparisons of the electrochemical and spectroscopic properties between the cyclometalated and noncyclometalated ruthenium complexes with the same bridging ligand are still rare. In this manuscript, we report on 2,3-di-2-pyridyl-5,6-diphenylpyrazine (dpdpz, **1**; Figure 1), as a new bridging ligand, and its complexation with ruthenium atoms. This ligand was designed so that it could behave as either a cyclometalating or a noncyclometalating ligand for ruthenium atoms. The difference between tppz and dpdpz is that two of the lateral pyridines in tppz are replaced by two phenyl rings in dpdpz. Compared to tppz, which has two N^N^N-type tridentate coordination sites, dpdpz is expected to bind transition metals in a C^N^N-type tridentate fashion to form cyclometalated complexes,[8] if the phenyl rings participate in the coordination with metals. However, if the phenyl rings remain intact, dpdpz could behave as a N^N-type bidentate binding ligand. It should be mentioned that a similar bridging ligand, dibenzo[*a*:*c*](dipyrido[2,3-*h*:2′,3′-*j*])phenazine ($dbdpzH_2$), was reported a few years ago.[9] However, attempts to prepare a symmetric dicyclometalated diruthenium complex were not successful.

Results and Discussion

Synthesis. 1 has been reported as a spectrophotometric reagent for copper and iron ions by Khuhawar and co-workers.[10] However, to the best of our knowledge, only limited studies on the synthesis and characterization of its transition-metal complexes have been described. **1** was readily prepared from the condensation of *meso*-1,2-diphenylethylenediamine with 2,2′-pyridil and subsequent dehydrogenation (Scheme 1). The precipitate, which was separated from the reaction mixture, was analytically pure and used for subsequent transformations without further purification. The reaction of **1** with 1 equiv of (tpy)$RuCl_3$ (tpy = 2,2′:6′,2″-terpyridine) in the presence of AgOTf gave the desired cyclometalated monoruthenium complex **2** in moderate yield (52%). When **1** was treated with 2 equiv of (tpy)$RuCl_3$, the biscyclometalated diruthenium complex **3** was isolated in 36% yield after flash column chromatography.

The reaction of 2 equiv of *cis*-$(bpy)_2RuCl_2$ (bpy = 2,2′-bipyridine) with dpdpz under microwave irradiation gave a mixture of monoruthenium complex **4** and diruthenium complex **5**. In this case, the dpdpz ligand coordinates to Ru^{II} atoms in a N^N bidentate fashion. After purification through flash column chromatography, **4** and **5** were obtained in 28% and 36% yield, respectively. Alternatively, monoruthenium complex **4** was prepared from 1 equiv of *cis*-$(bpy)_2RuCl_2$ and dpdpz in good yield (90%). The identities of **2**−**5** were confirmed by their ^{1}H NMR and mass spectrometry (MS) spectra and elemental analyses.

(3) (a) Balzani, V.; Campagna, S.; Denti, G.; Juris, A.; Serroni, S.; Venturi, M. *Acc. Chem. Res.* **1998**, *31*, 26. (b) Serroni, S.; Juris, A.; Campagna, S.; Venturi, M.; Denti, G.; Balzani, V. *J. Am. Chem. Soc.* **1994**, *116*, 9086. (c) Waterland, M. R.; Flood, A.; Gordon, K. C. *J. Chem. Soc., Dalton Trans.* **2000**, 121. (d) Denti, G.; Campagna, S.; Sabatino, L.; Serroni, S.; Ciano, M.; Balzani, V. *Inorg. Chem.* **1990**, *29*, 4750. (e) Serroni, S.; Denti, G.; Campagna, S.; Juris, A.; Ciano, M.; Balzani, V. *Angew. Chem., Int. Ed.* **1992**, *31*, 1493. (f) D'Alessandro, D. M.; Dinolfo, P. H.; Davis, M. S.; Hupp, J. T.; Keene, F. R. *Inorg. Chem.* **2006**, *45*, 3261. (g) Sahai, R.; Morgan, L.; Rillema, D. P. *Inorg. Chem.* **1988**, *27*, 3495. (h) Yoblinski, B. J.; Stathis, M.; Guarr, T. F. *Inorg. Chem.* **1992**, *31*, 5. (i) Richter, M. M.; Brewer, K. J.; Yoblinski, B. J.; Stathis, M.; Guarr, T. F. *Inorg. Chem.* **1992**, *31*, 1594. (j) Richter, M. M.; Brewer, K. J. *Inorg. Chem.* **1993**, *32*, 2827. (k) Milkevitch, M.; Brauns, E.; Brewer, K. J. *Inorg. Chem.* **1996**, *35*, 1737. (l) Marcaccio, M.; Paolucci, F.; Paradisi, C.; Roffia, S.; Fontanesi, C.; Yellowlees, L. J.; Serroni, S.; Campagna, S.; Denti, G.; Balzani, V. *J. Am. Chem. Soc.* **1999**, *121*, 10081. (m) Molnar, S. M.; Neville, K. R.; Jensen, G. E.; Brewer, K. J. *Inorg. Chim. Acta* **1993**, *206*, 69. (n) Braunstein, C. H.; Baker, A. D.; Strekas, T. C.; Gafney, H. D. *Inorg. Chem.* **1984**, *23*, 857.

(4) (a) Han, F. S.; Higuchi, M.; Kurth, D. G. *J. Am. Chem. Soc.* **2008**, *130*, 2073. (b) Collin, J.-P.; Lainé, P.; Launay, J.-P.; Sauvage, J.-P.; Sour, A. *Chem. Commun.* **1993**, 434. (c) Han, F. S.; Higuchi, M.; Kurth, D. G. *Org. Lett.* **2007**, *9*, 559. (d) Kaim, W.; Sarkar, B. *Coord. Chem. Rev.* **2007**, *251*, 584. (e) Carlson, C. N.; Kuehl, C. J.; Da Re, R. E.; Veauthier, J. M.; Schelter, E. J.; Milligan, A. E.; Scott, B. L.; Bauer, E. D.; Thompson, J. D.; Morris, D. E.; John, K. D. *J. Am. Chem. Soc.* **2006**, *128*, 7230. (f) Sauers, A. L.; Ho, D. M.; Bernhard, S. *J. Org. Chem.* **2004**, *69*, 8910.

(5) Coudret, C.; Fraysse, S.; Launay, J.-P. *Chem. Commun.* **1998**, 663.

(6) (a) Constable, E. C.; Thompson, A. M. W.; Greulich, S. *Chem. Commun.* **1993**, 1444. (b) Beley, M.; Collin, J.-P.; Louis, R.; Metz, B.; Sauvage, J.-P. *J. Am. Chem. Soc.* **1991**, *113*, 8521. (c) Lai, S.-W.; Cheung, T.-C.; Chan, M. C. W.; Cheung, K.-K.; Peng, S.-M.; Che, C.-M. *Inorg. Chem.* **2000**, *39*, 255. (d) Patoux, C.; Launay, J.-P.; Beley, M.; Chodorowski-Kimmers, S.; Collin, J.-P.; James, S.; Sauvage, J.-P. *J. Am. Chem. Soc.* **1998**, *120*, 3717. (e) Yao, C.-J.; Sui, L.-Z.; Xie, H.-Y.; Xiao, W.-J.; Zhong, Y.-W.; Yao, J. *Inorg. Chem.* **2010**, *49*, 8347. (f) Vilà, N.; Zhong, Y.-W.; Henderson, J. C.; Abruña, H. D. *Inorg. Chem.* **2010**, *49*, 796.

(7) (a) Duati, M.; Tasca, S.; Lynch, F. C.; Bohlen, H.; Vos, J. G.; Stagni, S.; Ward, M. D. *Inorg. Chem.* **2003**, *42*, 8377. (b) Duati, M.; Fanni, S.; Vos, J. G. *Inorg. Chem. Commun.* **2000**, *3*, 68.

(8) (a) Djukic, J.-P.; Sortais, J.-B.; Barloy, L.; Pfeffer, M. *Eur. J. Inorg. Chem.* **2009**, 817. (b) Jäger, M.; Smeigh, A.; Lombeck, F.; Görls, H.; Collin, J.-P.; Sauvage, J.-P.; Hammarström, L.; Johansson, O. *Inorg. Chem.* **2010**, *49*, 374. (c) Wadman, S. H.; Lutz, M.; Tooke, D. M.; Spek, A. L.; Hartl, F.; Havenith, R. W. A.; van Klink, G. P. M.; van Koten, G. *Inorg. Chem.* **2009**, *48*, 1887. (d) Wadman, S. H.; Havenith, R. W. A.; Hartl, F.; Lutz, M.; Spek, A. L.; van Klink, G. P. M.; van Koten, G. *Inorg. Chem.* **2009**, *48*, 5685. (e) Bomben, P. G.; Robson, K. C. D.; Sedach, P. A.; Berlinguette, C. P. *Inorg. Chem.* **2009**, *48*, 9631. (f) Koivisto, B. D.; Robson, K. C. D.; Berlinguette, C. P. *Inorg. Chem.* **2009**, *48*, 9644.

(9) Duprez, V.; Launay, J.-P.; Gourdon, A. *Inorg. Chim. Acta* **2003**, *343*, 395.

(10) Belcher, R.; Khuhawar, M. Y.; Stephen, W. I. *J. Chem. Soc. Pak.* **1989**, *11*, 185.

Scheme 1. Synthesis of the dpdpz Ligand **1** and Ruthenium Complexes **2**−**6**

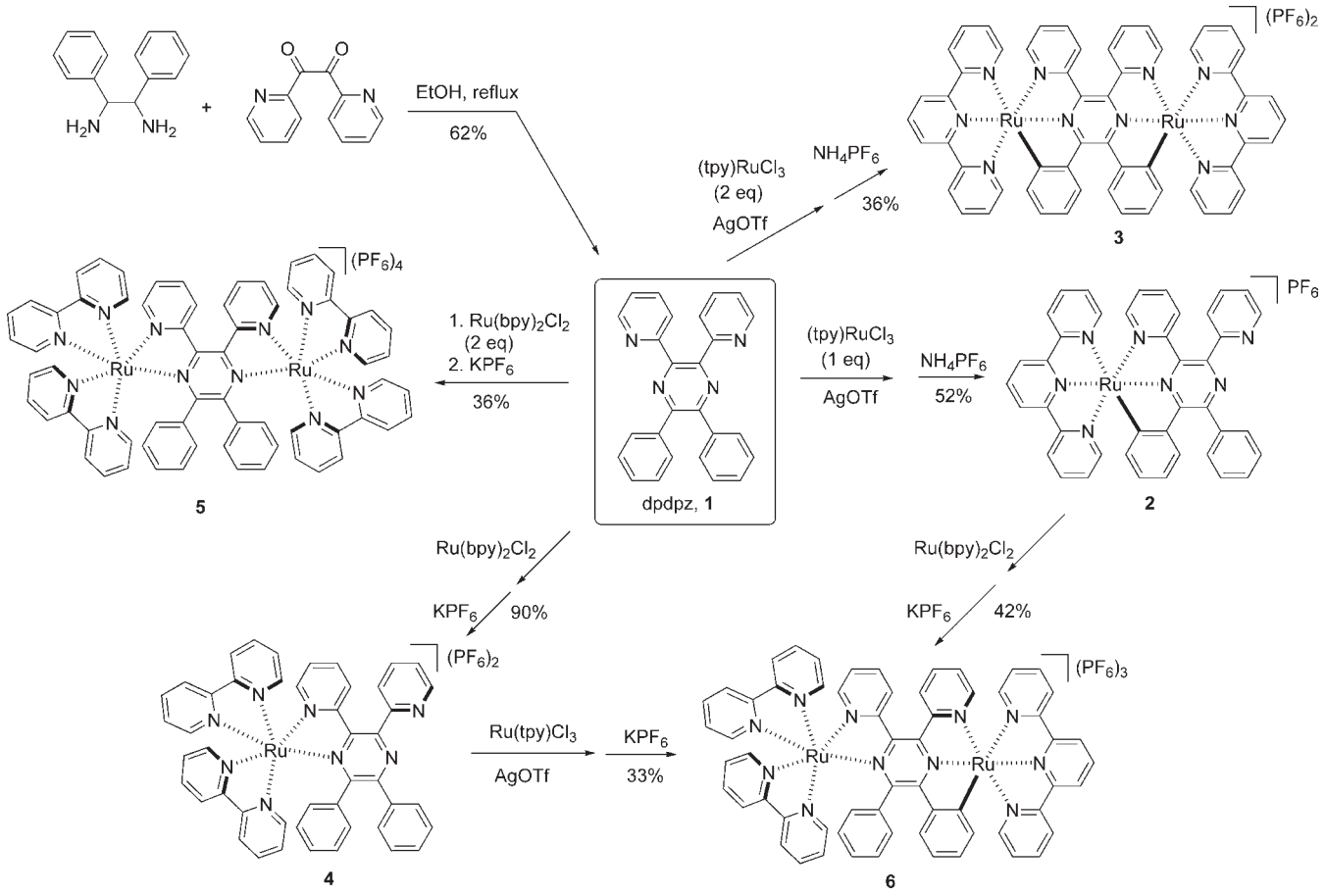

Judging from the ^{1}H NMR spectrum, diruthenium complex **5** was obtained as a mixture of two diastereomers (meso and rac) with a diastereoselectivity of 2:1. No attempts have been made to separate or distinguish these two diastereomers because the relative configuration of the ruthenium centers in similar diastereomers has a trivial effect on the luminescent and electrochemical properties.[11] The asymmetric diruthenium complex **6**, with one ruthenium being cyclometalated and another noncyclometalated, could be prepared from the reaction of either cyclometalated monoruthenium complex **2** with *cis*-$(bpy)_2RuCl_2$ or noncyclometalated monoruthenium complex **4** with $(tpy)RuCl_3$.

Electrochemical Studies. The electrochemical properties of complexes **2**−**6** were studied by cyclic voltammetry (CV). The CV profiles are shown in Figure 2, and their electrochemical data are summarized in Table 1, together with some related complexes for comparison. The anodic scan of **2** displays two redox couples at +0.67 and +1.31 V vs Ag/AgCl (entry 1). The former peak is assigned to the ruthenium-based II/III redox process, and the latter one could be attributed either to a $Ru^{III/IV}$ couple or to a ligand-based oxidative decomposition.[8] It is well-accepted that oxidation of the cyclometalated ruthenium atom takes place at much less positive potentials than noncyclometataed ruthenium centers, and this phenomenon could even be used to judge the formation of a Ru−C bond. For example, the $Ru^{II/III}$ redox process of $[(tpy)Ru(dbdpz)](PF_6)$ was reported to occur at +0.82 V vs SCE (entry 6).[9] The higher σ-donating character of the anionic carbon ligands, compared to a neutral nitrogen ligand, destabilizes the metal-centered HOMO level and, hence, gives a much lower oxidation potential. The cathodic scan of **2** shows two reversible redox couples at −1.33 and −1.71 V vs Ag/AgCl. The wave at −1.33 V is due to reduction of the dpdpz ligand, and reduction of tpy occurs at −1.71 V. As deduced from the CV data, the HOMO−LUMO energy gap of **2** is estimated to be 2.00 eV. In comparison, the tppz-bridged, noncyclometalated ruthenium analogue, $[(tpy)Ru(tppz)](PF_6)_2$ (entry 7), exhibits the first oxidation and reduction peaks at +1.50 and −0.95 V vs SCE, respectively, resulting in a HOMO−LUMO energy gap of 2.45 eV. We note that the cyclometalated complex has a much narrower energy gap, which could be advantageous for applications in molecular wires.

The CV profile of **3** displays two well-resolved redox couples at +0.65 and +0.84 V vs Ag/AgCl in the anodic scan (190 mV difference, entry 2), which suggests the presence of two Ru−C bonds in the complex and effective metal−metal electronic communication through the dpdpz bridging ligand. In addition, two irreversible processes were also observed at higher potentials. The comproportionation constant K_c for the equilibrium $Ru^{II}-Ru^{II} + Ru^{III}-Ru^{III} \leftrightarrow 2\ Ru^{II}-Ru^{III}$ is 1659, as determined by

(11) (a) Slater, J. W.; D'Alessandro, D. M.; Keene, F. R.; Steel, P. J. *Dalton Trans.* **2006**, 1954. (b) MacDonnell, F. M.; Kim, M.-J.; Wouters, K. L.; Konduri, R. *Coord. Chem. Rev.* **2003**, *242*, 47.

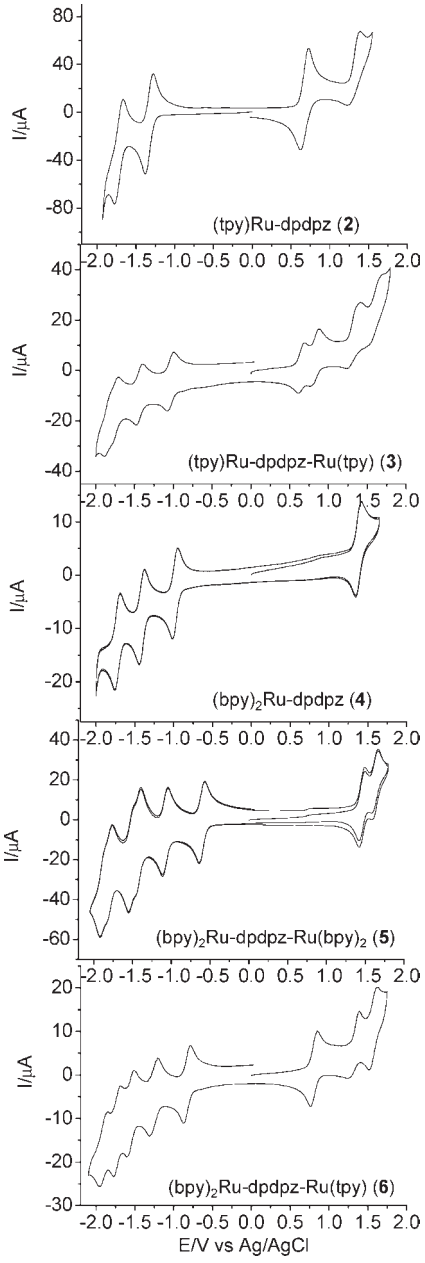

Figure 2. Cyclic voltammograms of complexes **2**−**6** in acetonitrile containing 0.1 M Bu_4NClO_4 at a scan rate of 100 mV/s. The working electrode is a glassy carbon, the counter electrode is a platinum wire, and the reference electrode is Ag/AgCl in saturated aqueous NaCl.

$K_c = 10^{\Delta E\,(mV)/59}$. The cathodic scan showed four couples at −1.03, −1.43, −1.73, and −1.86 V vs Ag/AgCl. The first two waves could be ascribed to reduction of the dpdpz ligand, and the latter two partially overlapped processes are from tpy. Coordination of the second ruthenium center makes the first reduction process of dpdpz 300 mV less negative because of a higher degree of electron delocalization of the dimetallic complex. The electrochemical energy gap is 1.68 eV for diruthenium complex **3**, which is 320 mV narrower relative to the ruthenium monomer **2**. This again reflects the significant effect of transition metals on the π-electron delocalization across the entire molecule. By comparing **3** with the tppz-bridged noncyclometalated diruthenium analogue, [(tpy)Ru(tppz)Ru(tpy)]-$(PF_6)_4$ (entry 8), which similarly shows six redox couples at +1.71, +1.40, −0.39, −0.86, −1.43, and −1.86 V (vs SCE; 310 mV difference in the two anodic waves and an energy gap of 1.79 eV), we can find that the cyclometalated complex, again, displays a narrower energy gap. However, the degree of metal−metal communication is weaker based on the potential separation of the formal potentials of the two anodic waves.

The noncyclometalated monoruthenium complex **4** displays one ruthenium-related reversible oxidation wave at +1.38 V vs Ag/AgCl and three ligand reduction waves at −0.97, −1.40, and −1.73 V (entry 3). The wave at −0.97 V is due to reduction of the dpdpz ligand, and waves at −1.40 and −1.73 V could be assigned to reduction of the two bpy ligands. The anodic scan of diruthenium complex **5** shows two well-resolved redox couples at +1.45 and +1.62 V vs Ag/AgCl (entry 4). The potential difference between these two waves is 170 mV, which again suggests strong metal−metal electronic communication through the dpdpz bridging ligand. The comproportionation constant K_c for the mixed-valence equilibrium is 761. The cathodic scan of **5** exhibited up to six redox couples at −0.60, −1.07, −1.42, −1.52, −1.79, and −1.89 V vs Ag/AgCl. The first two waves are due to reduction of the dpdpz ligand, and the latter four waves could be assigned to reduction of the four bpy ligands. The electrochemical energy gap, as determined from the potential gap between the first oxidation and first reduction wave in CV data, is 2.35 eV for **4** and 2.05 eV for **5**, respectively. The electrochemical properties of **4** and **5** are virtually the same as those of the dpp-bridged ruthenium monomer and dimer (entries 9 and 10), respectively.

It is interesting to take a closer look at the CV profile of the asymmetric diruthenium complex **6**, as shown in the bottom of Figure 2. The redox couple at +0.81 V is due to oxidation of the cyclometalated $Ru^{II/III}$ process, followed by an irreversible oxidation process at +1.32 V. The latter wave was assigned to either the cyclometalated $Ru^{III/IV}$ couple or the ligand-based oxidative decomposition based on its quasi-reversible nature[8] and as observed in the similar redox processes of cyclometalated complexes **2** and **3**. The redox couple at a more positive potential (+1.57 V) is likely from the noncyclometalated ruthenium center. It should be noted that the $Ru^{II/III}$ process of the cyclometalated ruthenium center of the asymmetric complex **6** occurs at a more positive potential than that of the first $Ru^{II/III}$ process of the symmetric biscyclometalated complex **3** (+0.81 vs +0.65 V). Moreover, the $Ru^{II/III}$ process of the noncyclometalated ruthenium center of **6** also takes place at a more positive potential than that of the first $Ru^{II/III}$ process of the symmetric bis-noncyclometalated complex **5** (+1.57 vs +1.45 V). This indicates the presence of electronic coupling between the two metal centers in the asymmetric diruthenium complex **6**. In the cathodic scan of **6**, five ligand-based redox couples were observed at −0.82, −1.25, −1.55, −1.73, and −1.90 V vs Ag/AgCl (entry 5). The first two waves are likely from reduction of the dpdpz ligand, and the latter three waves are due to reduction of the bpy and tpy ligands. By comparison of the first reduction potential of diruthenium complexes **3**, **5**, and **6** (−1.03, −0.60, and −0.82 V, respectively), it is evident that the bis-noncyclometalated complex **5** could be reduced at the least negative potential and the biscyclometalated complex **3** at the most negative potential.

Table 1. Electrochemical Data of Complexes **2**−**6** and Some Related Compounds[a]

			$E_{1/2}$(ligand-based)		
entry	complex	$E_{1/2}$(anodic)	bridging ligand	bpy or tpy	ΔE^b (eV)
1	**2**, [(tpy)Ru(dpdpz)](PF_6)	0.67, 1.31	−1.33	−1.71	2.00
2	**3**, [(tpy)Ru(dpdpz)Ru(tpy)]$(PF_6)_2$	0.65, 0.84, 1.33, 1.60	−1.03, −1.43	−1.73, −1.86	1.68
3	**4**, $[(bpy)_2Ru(dpdpz)](PF_6)_2$	1.38	−0.97	−1.40, −1.73	2.35
4	**5**, $[(bpy)_2Ru(dpdpz)Ru(bpy)_2](PF_6)_4$	1.45, 1.62	−0.60, −1.07	−1.42, −1.52, −1.79, −1.89	2.05
5	**6**, $[(bpy)_2Ru(dpdpz)Ru(tpy)](PF_6)_3$	0.81, 1.32, 1.57	−0.82, −1.25	−1.55, −1.73, −1.90	1.63
6	[(tpy)Ru(dbdpz)](PF_6)[c]	0.82	−1.07	−1.56, −1.62	1.89
7	[(tpy)Ru(tppz)]$(PF_6)_2$[d]	1.50	−0.95, −1.40	−1.60	2.45
8	[(tpy)Ru(tppz)Ru(tpy)]$(PF_6)_4$[d]	1.40, 1.71	−0.39, −0.86	−1.43, −1.86	1.79
9	$[(bpy)_2Ru(dpp)](PF_6)_2$[e]	1.38	−1.01	−1.49, −1.72	2.39
10	$[(bpy)_2Ru(dpp)Ru(bpy)_2](PF_6)_4$[e]	1.43, 1.61	−0.61, −1.09		2.04

[a] All measurements were carried out in acetonitrile containing 0.1 M Bu_4NClO_4 as the supporting electrolyte. Unless otherwise noted, the potential was reported as the $E_{1/2}$ value vs Ag/AgCl. [b] The electrochemical energy gap is determined by the potential difference between the first oxidation and first reduction wave. [c] $E_{1/2}$ vs SCE. See ref 9. [d] $E_{1/2}$ vs SSCE. See ref 2a. [e] $E_{1/2}$ vs SSCE. See ref 3m.

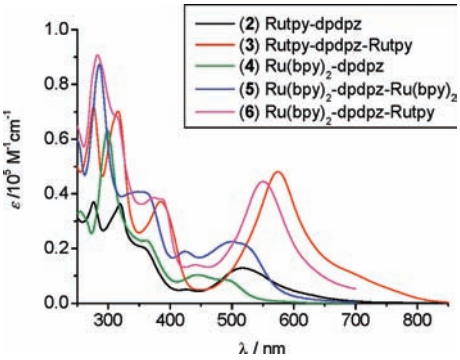

Figure 3. UV/vis absorption spectra of **2**−**6** in acetonitrile.

This is reasonable because complex **3** has two negatively charged ligands, which makes it difficult to reduce. The electrochemical energy gap of the asymmetric diruthenium complex **6** (1.63 eV) is similar to that of the biscyclometalated complex **3** (1.68 eV).

Electronic Absorption Spectroscopic Studies. The electronic absorption spectra of complexes **2**−**6** are shown in Figure 3, and the corresponding absorption maxima and molar absorption coefficients are presented in Table 2. Generally speaking, transitions in the UV region are largely due to intraligand $\pi-\pi^*$ excitations, while the intense and broad bands in the visible region are ascribed to metal-to-ligand charge-transfer (MLCT) transitions.[8] Monocyclometalated ruthenium complex **2** displayed a broad MLCT band centered at 515 nm (black line). This band could arise from the transition from ruthenium to the cyclometalating dpdpz ligand. In comparison, the corresponding MLCT band in biscyclometalated complex **3** appears much broader and more intense (red line), in addition to a large red shift compared to **2**. This reflects a greater degree of electron delocalization across the molecule in the case of the bimetallic complex, which correlates well with the electrochemical results described above. As far as the noncyclometalated monoruthenium complex **4** is concerned, two MLCT bands, centered at 446 and 490 nm, are evident in the visible region (olive line). They are assigned to the ruthenium to bpy and dpdpz ligand charge transfer, respectively. Because the dpdpz ligand is easier to reduce than bpy, as evidenced in the electrochemical studies, the MLCT band of dpdpz would be expected to be at lower energy. The peak at 299 nm is attributed to the ancillary bpy-based intraligand $\pi-\pi^*$ transition. The peak at 360 nm is likely from the intraligand transition of the dpdpz ligand. Complex **5**, with two noncyclometalated ruthenium atoms, exhibits multiple MLCT bands between 400 and 600 nm (blue line). On the other hand, the asymmetric diruthenium complex **6** shows an intense ruthenium-to-cyclometalating dpdpz ligand charge-transfer band at 550 nm (magenta line). This band is of similar intensity, albeit with a 24 nm blue shift, when compared to that of the symmetric biscyclometalated complex **3**. By comparison of all five spectra together, it is clear that the metal-to-cyclometalating ligand charge-transfer transition is much broader and more intense and red-shifted, as observed in either symmetric biscyclometalated complex **3** or asymmetric complex **6**. This property would make them good potential light-harvesting materials.

Emission Spectroscopic Studies. Among the five ruthenium complexes synthesized above, noncyclometalated complexes **4** and **5** are emissive at room temperature. No emission was detected from the cyclometalated complexes **2**, **3**, and **6** in a fluidic acetonitrile solution at room temperature, contrasting with the bis(triazole)- or bis(tetrazole)pyridine-based ruthenium complexes cited in ref 7. However, it might be possible that the photomultiplier tube employed (R928F) is not sufficiently red-sensitive to detect any low-energy weak emission from these complexes, if present. The emission spectra of **4** and **5** are presented in Figure 4, and the positions of the luminescence maxima are summarized in Table 2. Mononuclear ruthenium complex **4** exhibited a broad luminescence band with a maximum at 709 nm. The luminescence quantum yield of **4** was 0.057%. The emission spectral changes of **4** upon an increase in the acidity of the aqueous solution, by adding H_2SO_4, are shown in Figure 5. Clearly, protonation of the free nitrogen atom in **4** quenches its emission. The emission could be recovered by the addition of the appropriate amount of aqueous NaOH (Figure S4 in the Supporting Information). Similar results for ruthenium complexes containing dpp bridging ligands have been reported.[12] The weak band at 675 nm appears too narrow to be real, and it could be due to an instrumental

(12) (a) Hosek, W.; Tysoe, S. A.; Gafney, H. D.; Baker, A. D.; Strekas, T. C. *Inorg. Chem.* **1989**, *28*, 1228. (b) Nazeeruddin, M. K.; Kalyanasundaram, K. *Inorg. Chem.* **1989**, *28*, 4251.

Table 2. Absorption and Emission Data of Complexes **2**–**6** and Some Related Compounds[a]

entry	complex	absorption λmax/nm ($\varepsilon/10^5$ $M^{-1}cm^{-1}$)	emission[b] λ_{max}/nm (quantum yield)
1	**2**, $[(tpy)Ru(dpdpz)](PF_6)$	276 (0.37), 319 (0.37), 360 (0.20), 427 (0.053), 515 (0.13)	
2	**3**, $[(tpy)Ru(dpdpz)Ru(tpy)](PF_6)_2$	276 (0.71), 316 (0.70), 384 (0.37), 574 (0.48)	
3	**4**, $[(bpy)_2Ru(dpdpz)](PF_6)_2$	299 (0.63), 360 (0.23), 446 (0.10), 490 (0.088)	709 (0.057%)
4	**5**, $[(bpy)_2Ru(dpdpz)Ru(bpy)_2](PF_6)_4$	285 (0.87), 360 (0.41), 423 (0.19), 496 (0.22)	791 (0.023%)
5	**6**, $[(bpy)_2Ru(dpdpz)Ru(tpy)](PF_6)_3$	282 (0.91), 374 (0.39), 438 (0.14), 550 (0.44)	
6	$[Ru(bpy)_3](PF_6)_2$	285 (0.65), 354 (0.051), 420 (0.087), 455 (0.11)	612 (5.9%)
7[c]	$[(bpy)_2Ru(dpp)](PF_6)_2$	430 (0.12), 470	675 (5.1%)
8[c]	$[(bpy)_2Ru(dpp)Ru(bpy)_2](PF_6)_4$	425 (0.17), 525 (0.21)	755 (0.31%)

[a] All spectra were recorded in a conventional 1.0 cm quartz cell in acetonitrile. [b] The excitation wavelength is 400 nm. The quantum yield is calculated by comparing it with a standard sample $[Ru(bpy)_3](PF_6)_2$, which has a quantum yield of 5.9% in N_2-saturated acetonitrile. [c] See ref 3n.

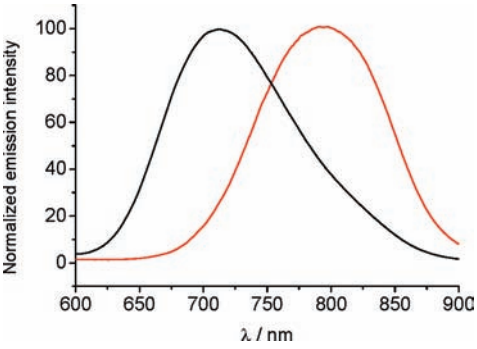

Figure 4. Normalized emission spectra of complexes **4** (black line) and **5** (red line) in acetonitrile. The excitation wavelength was 400 nm.

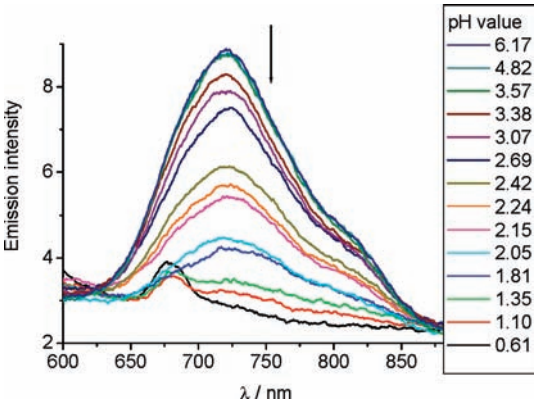

Figure 5. Emission spectral changes of monoruthenium complex **4** at different pH values in water. The excitation wavelength was 400 nm. The weak bands at 675 and 820 nm are due to an instrumental artifact.

artifact. From the emission titration in Figure 5, the pK_a value for the excited state of the protonated **4** was calculated to be 2.5 (see the Supporting Information for details).

When the second ruthenium atom is coordinated to **4**, the emission of the resulting dinuclear complex **5** moves into the NIR region, displaying a broad luminescence band with a maximum between 700 and 880 nm, albeit with a lower quantum yield of 0.023%. It should be noted that both of the above emission spectra are independent of the excitation wavelength, and the quantum yield is around 15% less in an air-purged solution. As far as the asymmetric dinuclear complex **6** is concerned, attachment of the cyclometalated ruthenium component leads to the complete disappearance of emission, which we believe is the result of fast energy transfer from the excited state of the noncyclometalated ruthenium component to

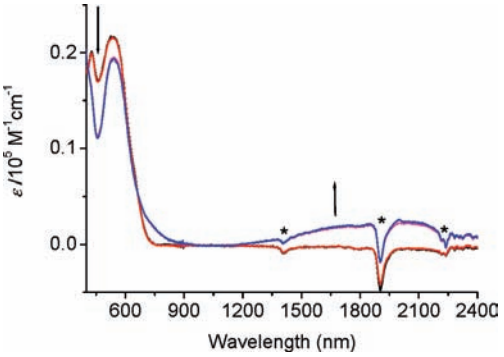

Figure 6. Absorption spectral changes of diruthenium complex **5** upon electrolysis at +1.55 V vs Ag/AgCl in CD_3CN containing 0.1 M n-Bu_4NClO_4. Asterisks indicate artifacts due to errors in compensation of solvent absorption.

the low-lying and nonradiative cyclometalated ruthenium moiety state.[13]

Spectroelectrochemical Studies. Studies of mixed-valence dimetallic complexes have attracted much attention.[14] These studies are pertinent to the understanding of naturally occurring electron-transfer processes and molecular electronics. As mentioned in the previous sections, symmetric diruthenium complexes **3** and **5** displayed large differences in the formal potentials ($\Delta E^{\circ\prime}$), suggesting the presence of strong electronic communication between the two metal centers in these complexes. To further probe the electronic coupling between ruthenium atoms, spectroelectrochemical measurements were carried out. Upon electrolysis of the bis-noncyclometalated complex **5** at +1.55 V vs Ag/AgCl at a platinum mesh electrode (Figure 6), partial diminution of the visible MLCT band intensity was evident along with the concomitant emergence of a broad band centered at 1920 nm (5200 cm^{-1}). Upon further electrolysis at +1.80 V, this band disappeared (Figure S5 in the Supporting Information). This NIR band could be assigned to an intervalence charge-transfer (IVCT) transition of the in situ generated mixed-valence complex. The observed full width at half-height ($\Delta\nu_{1/2}$) was 2900 cm^{-1}, which is narrower than, although of the same order of magnitude as, the theoretical value of 3465 cm^{-1}, as calculated from the Hush formula $\Delta\nu_{1/2} = (2310\nu_{max})^{1/2}$ for

(13) Ott, S.; Borgström, M.; Hammarström, L.; Johansson, O. *Dalton Trans.* **2006**, 1434.

(14) (a) D'Alessandro, D. M.; Keene, F. R. *Chem. Rev.* **2006**, *106*, 2270. (b) Demadis, K. D.; Hartshorn, C. M.; Meyer, T. J. *Chem. Rev.* **2001**, *101*, 2655. (c) Kaim, W.; Lahiri, G. K. *Angew. Chem., Int. Ed.* **2007**, *46*, 1778. (d) Chisholm, M. H.; Patmore, N. J. *Acc. Chem. Res.* **2007**, *40*, 19. (e) Kaim, W.; Klein, A.; Glöckle, M. *Acc. Chem. Res.* **2000**, *33*, 755. (f) D'Alessandro, D. M.; Keene, F. R. *Chem. Soc. Rev.* **2006**, *35*, 424. (g) Launay, J.-P. *Chem. Soc. Rev.* **2001**, *30*, 386.

weakly or moderately coupled class II mixed-valence systems.[15] The electronic coupling parameter H_{ab} is calculated to be 650 cm^{-1}, according to the Hush formula:[16] $H_{ab} = 2.06 \times 10^{-2}(\varepsilon_{max}\nu_{max}\Delta\nu_{1/2})^{1/2}/r_{ab}$, where ε_{max} equals 0.031×10^5 M^{-1} cm^{-1}, ν_{max} equals 5200 cm^{-1}, $\Delta\nu_{1/2}$ equals 2900 cm^{-1}, and r_{ab} is estimated to be 6.85 Å according to a reported crystal structure of a similar diruthenium complex bridged by dpb.[17] One-electron oxidation of biscyclometalated complex **3** at +0.76 V vs Ag/AgCl did not give rise to a distinct IVCT band in the NIR region (Figure S6 in the Supporting Information). Another possibility is that it could be too broad and weak, if indeed present, to be clearly discerned.

Conclusions

In summary, the dpdpz ligand, described in this contribution, was found to be a versatile bridging ligand for the synthesis of new transition-metal complexes with implications in molecular wires and the construction of more sophisticated supramolecular systems and architectures. This ligand could be readily prepared in a one-step reaction from commercially available starting materials. It is of great interest that dpdpz can bind to ruthenium atoms with different coordination modes, namely, in a N^N-type bidentate fashion or in a C^N^N tridentate mode, to form a metallacycle. We have prepared five dpdpz-containing mononuclear and dinuclear ruthenium complexes, and each metal could be cyclometalated or noncyclometalated. Combined electrochemical and spectroscopic studies showed that these complexes exhibit intriguing structural and electronic features. In comparison, cyclometalated complexes have rigid linear conformation, narrower energy gaps, and lower formal potentials of the metal centers. These properties make them potential candidates as molecular wires and as light-harvesting materials. Noncyclometalated complexes were found to emit at room temperature. However, attachment of a cyclometalated ruthenium atom completely quenched the emission. This behavior would make the asymmetric diruthenium complex a good candidate for the dynamic study of fast energy-transfer processes. Future work will focus on the preparation and application of new complexes based on dpdpz and related ligands.

Experimental Section

Spectroscopic Measurements. All optical UV/vis absorption spectra were obtained using a TU-1810DSPC spectrometer of Beijing Purkinje General Instrument Co. Ltd. at room temperature in denoted solvents, with a conventional 1.0 cm quartz cell. Emission spectra were recorded using a F-380 spectrofluorimeter of Tianjin Gangdong Sic. & Tech Development Co. Ltd., with a red-sensitive photomultiplier tube R928F. Samples for emission measurement were obtained in quartz cuvettes of 1 cm path length. Luminescence quantum yields were determined using $[Ru(bpy)_3](PF_6)_2$ in a degassed acetonitrile solution as the standard (ϕ = 5.9%);[18] the estimated uncertainty of ϕ is ±10% or better.

Electrochemical Measurements. All CV was taken using an Epsilon BAS CV-27 or a CHI620D potentiostat. One-compartment electrochemical cells with a provision for gas addition were employed. A glassy carbon electrode with a diameter of 3 mm was used as the working electrode. The electrode was polished prior to use with 1 μm diamond paste (Buehler) and rinsed thoroughly with water and acetone. A large-area platinum wire coil was used as the counter electrode. All potentials were referenced to a saturated Ag/AgCl electrode without regard for the liquid junction potential. All measurements were carried out with a 0.3 mM concentration of the corresponding complex in acetonitrile at a scan rate of 100 mV/s, with 0.1 M Bu_4NClO_4 as the supporting electrolyte.

Synthesis. All reactions were carried out under an atmosphere of dry nitrogen using standard Schlenk techniques. Dry tetrahydrofuran was distilled from sodium/benzophenone, and other solvents (analytical grade) were used without further purification. NMR spectra were recorded in the designated solvent on a Varian 300 or Varian 400 spectrometer. MALDI-TOF positive-ion data were obtained with a Waters MALDI micro-MX mass spectrometer run in a reflection mode. Cyclometalated complexes were synthesized followed by a published procedure with slight modifications (see ref 9).

2,3-Di-2-pyridyl-5,6-diphenylpyrazine (dpdpz, 1). A solution of *meso*-1,2-diphenylethylenediamine (42 mg, 0.2 mmol) and 2,2′-pyridil (42 mg, 0.2 mmol) in 5 mL of ethanol was refluxed for 24 h under a N_2 atmosphere. After cooling, the mixture was open to air and stirred for another 2 days at room temperature. The yellow precipitate was collected after filtration to give 50 mg of product with a yield of 62%. ^{1}H NMR (300 MHz, $CDCl_3$): δ 7.20−7.26 (m, 2H), 7.30−7.35 (m, 6H), 7.58−7.62 (m, 4H), 7.80 (t, J = 7.5 Hz, 2H), 8.08 (d, J = 7.8 Hz, 2H), 8.36 (d, J = 3.9 Hz, 2H). ESI-HRMS. Calcd for $[M + H]^+$: m/z 387.1610. Found: m/z 387.1613. Anal. Calcd for $C_{26}H_{18}N_4$: C, 80.81; H, 4.69; N, 14.50. Found: C, 80.79; H, 4.59; N, 14.47.

[(tpy)Ru(dpdpz)](PF$_6$) (2). To a solution of $(tpy)RuCl_3$ (44 mg, 0.10 mmol) in 30 mL of acetone was added 91 mg (0.35 mmol) of AgOTf, and the mixture was refluxed for 2 h. After cooling to room temperature, the mixture was filtered through a pad of Celite, and then concentrated under reduced pressure. To the residue were then added the dpdpz ligand **1** (39 mg, 0.10 mmol), 10 mL of *N*, *N*-dimethylformamide (DMF), and ^{t}BuOH, respectively. The resulting mixture was refluxed for another 20 h before cooling and removal of some insoluble impurities through filtering. The solvent was removed at reduced pressure. The residue was dissolved in 10 mL of MeOH, and then excess NH_4PF_6 was added. The precipitate generated was collected and purified through flash column chromatography on silica gel to give 45 mg of **2** as a brownish solid in a yield of 52%. ^{1}H NMR (300 MHz, CD_3CN): δ 5.84 (dd, J = 7.5 and 1.5 Hz, 1H), 6.40 (td, J = 7.8 and 1.5 Hz, 1H), 6.48 (td, J = 7.2 and 1.5 Hz, 1H), 7.05 (m, 2H), 7.14 (m, 2H), 7.34 (d, J = 9.0 Hz, 1H), 7.51 (m, 2H), 7.62 (m, 6H), 7.83 (td, J = 7.80 and 1.5 Hz, 2H), 7.90 (m, 2H), 8.18 (m, 3H), 8.46 (d, J = 8.4 Hz, 2H), 8.67 (d, J = 7.8 Hz, 2H), 8.70 (m, 1H, overlapped). MALDI-MS: 720 ($[M - 2PF_6]^{2+}$). Anal. Calcd for $C_{41}H_{28}F_6N_7PRu$: C, 56.95; H, 3.26; N, 11.34. Found: C, 56.71; H, 3.16; N, 11.09.

[(tpy)Ru(dpdpz)Ru(tpy)](PF$_6$)$_2$ (3). To a solution of $(tpy)RuCl_3$ (90 mg, 0.21 mmol) in 30 mL of acetone was added 195 mg (0.70 mmol) of AgOTf, and the mixture was refluxed for 2 h. After cooling to room temperature, the mixture was filtered through a pad of Celite and then concentrated under reduced pressure. To the residue were then added the dpdpz ligand **1** (39 mg, 0.10 mmol), 15 mL of DMF, and ^{t}BuOH, respectively. The resulting mixture was refluxed for another 20 h before cooling and removal of some insoluble impurities through filtering. The solvent was removed at reduced pressure. The residue was dissolved in 10 mL of MeOH, and then excess NH_4PF_6 was added. The precipitate generated was collected after filtering and purified through flash column chromatography on silica gel to give 49 mg of **3** as a purple solid in a yield of 36%. ^{1}H NMR (300 MHz, CD_3CN): δ 6.02 (dd, J = 7.5 and 1.5 Hz, 2H), 6.67 (m, 4H), 7.23 (m, 6H), 7.70−7.90 (m, 12H), 8.23 (t, J = 8.1 Hz, 2H), 8.36 (dd, J = 7.8 and 1.5 Hz, 2H), 8.52 (d, J = 8.4 Hz, 4H), 8.72 (d, J = 7.8 Hz, 6H). MALDI-MS: 1054 ($[M - 2PF_6]^{2+}$), 720

(15) (a) Hush, N. S. *Prog. Inorg. Chem.* **1967**, *8*, 391. (b) Hush, N. S. *Electrochim. Acta* **1968**, 1005.
(16) Hush, N. S. *Coord. Chem. Rev.* **1985**, *64*, 135.
(17) D'Alessandro, D. M.; Junk, P. C.; Keene, F. R. *Supramol. Chem.* **2005**, *17*, 529.
(18) Nakamura, K. *Bull. Chem. Soc. Jpn.* **1982**, *55*, 1639.

([M − 2PF_6 − Ru − tpy]$^+$). Anal. Calcd for $C_{56}H_{38}F_{12}N_{10}P_2Ru_2\cdot Et_2O$: C, 50.85; H, 3.41; N, 9.88. Found: C, 50.82; H, 3.32; N, 10.08.

[(bpy)$_2$Ru(dpdpz)](PF$_6$)$_2$ (4). To a solution of dpdpz (193 mg, 0.50 mmol) in 25 mL of ethylene glycol was added 260 mg of $Ru(bpy)_2Cl_2\cdot 2H_2O$[19] (0.50 mmol), and the mixture was heated under microwave irradiation for 30 min. After cooling to room temperature, an excess of an aqueous solution of KPF_6 was added. The precipitate generated was collected and purified through flash column chromatography on silica gel to give 488 mg of **4** as a deep-yellow solid in 90% yield. ^{1}H NMR (400 MHz, CD_3CN): δ 6.01 (d, J = 7.5 Hz, 1H), 6.45 (t, J = 7.4 Hz, 1H), 6.72 (t, J = 6.5 Hz, 1H), 6.83 (d, J = 5.5 Hz, 1H), 6.88−6.94 (m, 2H), 7.16 (t, J = 7.5 Hz, 2H), 7.22 (d, J = 7.3 Hz, 5H), 7.33 (d, J = 5.4 Hz, 1H), 7.41 (t, J = 8.7 Hz, 2H), 7.54−7.67 (m, 6H), 7.93−7.98 (m, 2H), 8.13−8.19 (m, 3H), 8.25 (d, J = 7.7 Hz, 1H), 8.30 (d, J = 5.4 Hz, 1H), 8.38 (t, J = 7.6 Hz, 2H), 8.50 (d, J = 8.1 Hz, 1H), 8.56 (d, J = 5.5 Hz, 1H), 8.61 (d, J = 4.6 Hz, 1H). ESI-MS. Calcd for [M−PF_6]$^+$: m/z 945.3. Anal. Calcd for $C_{46}H_{34}N_8P_2F_{12}Ru\cdot H_2O$: C, 49.87; H, 3.28; N, 10.11. Found: C, 49.87; H, 3.17; N, 9.67.

[(bpy)$_2$Ru(dpdpz)Ru(bpy)$_2$](PF$_6$)$_4$ (5). To a solution of dpdpz (38.6 mg, 0.10 mmol) in 10 mL of ethylene glycol was added 103 mg of $Ru(bpy)_2Cl_2\cdot 2H_2O$ (0.20 mmol). The mixture was heated under microwave irradiation for 20 min. After cooling to room temperature, an excess of an aqueous solution of KPF_6 was added. The precipitate generated was collected and purified through flash column chromatography on silica gel to afford 65.5 mg of **5** as a brownish solid in a yield of 36%. Because of the presence of a mixture of diastereomers, it is difficult to assign the ^{1}H NMR signals. However, it is evident from the spectrum that two diastereomers exist in a rough ratio of 2:1. MALDI-MS: 1503.0 ([M − 2PF_6 −H]$^{2+}$). Anal. Calcd for $C_{66}H_{50}F_{24}N_{12}P_4Ru_2\cdot H_2O$: C, 43.77; H, 2.89; N, 9.28. Found: C, 43.70; H, 2.95; N, 9.22.

[(bpy)$_2$Ru(dpdpz)Ru(tpy)](PF$_6$)$_3$ (6). To a solution of $(tpy)RuCl_3$[20] (35 mg, 0.08 mmol) in 30 mL of acetone was added 73 mg of AgOTf (0.28 mmol). The mixture was refluxed for 2 h under N_2. After cooling to room temperature, the generated AgCl precipitate was removed by filtering through Celite. The filtrate was then concentrated under reduced pressure. To the residue were added mono-ruthenium complex **2** (87 mg, 0.08 mmol), 10 mL of DMF, and ^{t}BuOH, respectively. The resulting mixture was refluxed under a N_2 atmosphere for another 24 h before cooling and removal of the solvent under reduced pressure. The residue was dissolved in 5 mL of MeOH, followed by the addition of 15 mL of water and an excess of KPF_6. The precipitate generated was collected after filtering and purified through flash column chromatography on silica gel to give 41 mg of **6** as a deep-purple solid in a yield of 33%. MALDI-MS: 1423.9 ([M − H − PF_6]$^+$), 1278.0 ([M − 2PF_6]$^{2+}$), 976.2 ([M − 2H − bpy −3PF_6]$^{3+}$). Anal. Calcd for $C_{61}H_{44}F_{18}N_{11}P_3Ru_2\cdot 2H_2O$: C, 45.67; H, 3.02; N, 9.60. Found: C, 45.46; H, 2.83; N, 9.83.

Acknowledgment. We thank the Institute of Chemistry, Chinese Academy of Sciences ("100 Talent" Program), and the National Natural Science Foundation of China (Grant 21002104) for funding support. This work was also supported by the Center for Molecular Interfacing, an NSF Phase I Center for Chemical Innovation award (0847926), and the Cornell Center for Materials Research.

Supporting Information Available: pH titration and pK_a* determination of **4**, absorption and emission spectral changes of complex **4** at different pH values in water, spectroelectrochemical analysis of **5** and **3**, and NMR and MS spectra of new compounds. This material is available free of charge via the Internet at http://pubs.acs.org.

(19) Sullivan, B. P.; Salmon, D. J.; Meyer, T. J. *Inorg. Chem.* **1978**, *17*, 3334.

(20) Sullivan, B. P.; Calvert, J. M.; Meyer, T. J. *Inorg. Chem.* **1980**, *19*, 1404.